Applied Ocean Research 42 (2013) 55–59

Contents lists available at SciVerse ScienceDirect

Applied Ocean Research

journal homepage: www.elsevier.com/locate/apor

Premature refusal of large-diameter, deep-penetration piles on an offshore platform

Li Sa[a,*], Tian Yinghui[b], Zhou Yangrui[c], Jiang Baofan[c], Wang Jinbiao[a]

[a] The Civil Engineering Department, Tianjin University, Tianjin, China
[b] Center for Offshore Foundation System, The University of Western Australia, Perth, Australia
[c] China Oilfield Services Limited, Tianjin, China

ARTICLE INFO

Article history:
Received 9 May 2012
Received in revised form 17 March 2013
Accepted 12 April 2013

Keywords:
Offshore pile
Pile driving
Premature refusal
Soil setup
Soil resistance to driving

ABSTRACT

Open-ended pipe piles are commonly driven into the seabed to support offshore platforms. This paper presents a case of practical offshore driven pile installation experiences associating with premature refusal. Pile drivability and capacity are analyzed using sufficient driving records. Dynamic loading tests were performed three months after the driving in order to determine the pile capacity after refusal. The test results are detailed in this paper compared with back analysis of measured pile driving records. Empirical equations are provided to predict soil resistance during driving and after setup according to the driving records and dynamic loading tests. Analyzing this practical engineering case is hoped to lead to a better understanding of pile driving, especially when premature refusal occurs. The sufficient details of the engineering data in this paper are also expected to enrich the engineering experience and literature of offshore piles in offshore engineering.

1. Introduction

Steel jacket structures are still the most common form of fixed offshore platforms, which are fixed to the seabed by piles inserted through sleeves attached to the jacket and the piles are eventually grouted to the sleeves after installation. One of the most common construction problems for driven piles is associated with the incorrect choice of design penetration, resulting in either insufficient bearing capacity or premature refusal [1]. Examples of premature refusal and associating collapse of pile tip were reported in the literature [2–4]. Removal of the soil plug inside the pile by drilling or jetting is normally required in this scenario in order to further drive the pile to reach the targeted depth, which will inevitably increase the cost significantly and delay the project completion [5].

Up to now, considerable amount of studies have been conducted from different perspectives to understand pile drivability and associated issues. Brunning and Ishak [6] tried to improve reliability of the pile driving predictions in carbonate soils and rock based on installation data in Timor Sea. Mohamad et al. [7] studied the effects of high-rebound of soil on pile drivability using static and dynamic tests. In addition, cone penetration tests (CPT) were highly recommended to make prediction of pile drivability in recent years [8,9]. All these available studies have shown that there are many factors affecting pile drivability, such as the hammer driving system characteristics, pile type, size and length and soil resistance behavior. According to Stevens [10], premature refusal is likely due to significant end bearing in granular soils or soil setup, i.e. the time-dependent change in pile capacity.

Although the state-of-the-art approaches have allowed significant advances in the analysis of the problem, the understanding of pile–soil interactions during pile installation is still quite limited. The majority of the current design approaches are still empirical based [11]. High-quality information, especially associating with practical engineering projects, on large-diameter, deep-penetration piles is difficult to find in the literature.

This paper presents sufficient details of a real engineering project with premature refusal occurring, including pile driving records, retrospective analysis and dynamic testing 3 months after the refusal. These practical data and recorded information were analyzed toward a better understanding of the pile–soil behavior.

2. Overview of the project

A jacket platform with a 2000-ton steel substructure designed to support a 8000-ton integrated deck has been built in the Nanbao oil field in the Bohai Bay of China. The water depth of this project is 14 m. The platform foundation consists of 6 individual piles with a uniform outer diameter of 1.524 m. The design length of the piles is about 128 m and the penetration depth below mudline is designed to be 104 m. The wall thickness of the piles is 38.1 mm except that a 1.5 m long pile shoe has a 50.8 mm thickness.

* Corresponding author. Tel.: +86 022 27428932.
E-mail address: lisa@tju.edu.cn (L. Sa).

0141-1187/$ - see front matter © 2013 Elsevier Ltd. All rights reserved.
http://dx.doi.org/10.1016/j.apor.2013.04.002

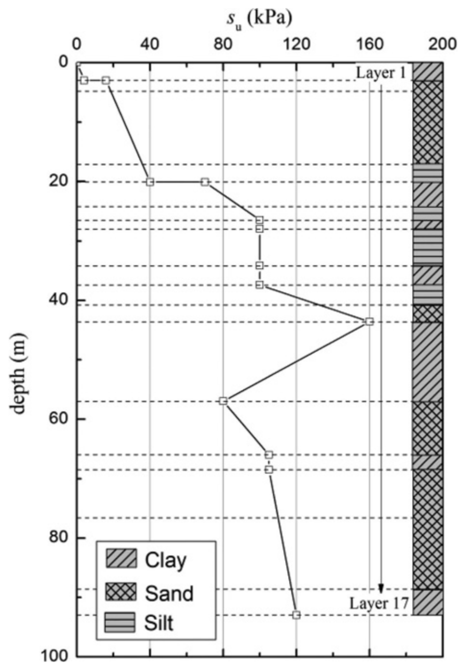

Fig. 1. Soil undrained shear strength.

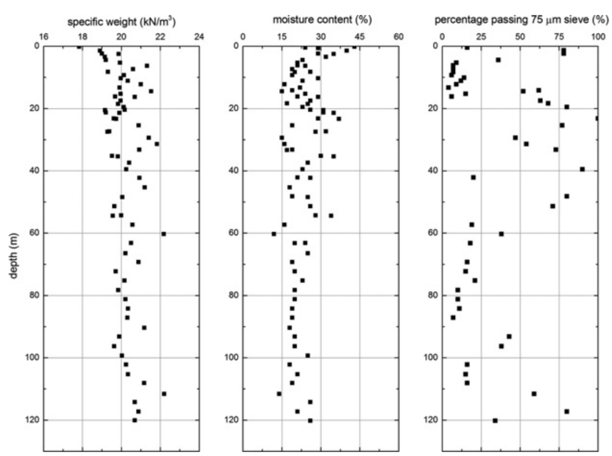

Fig. 2. Soil parameters.

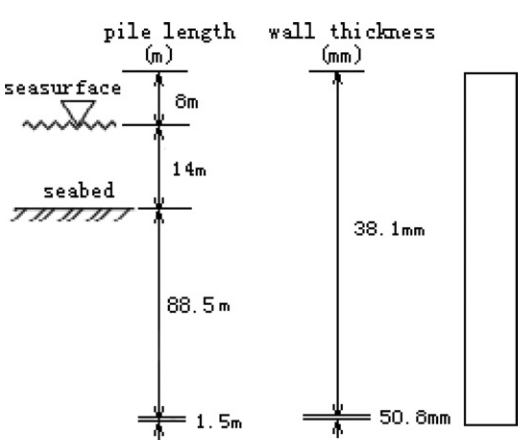

Fig. 3. Pile calculation model for wave equation analysis.

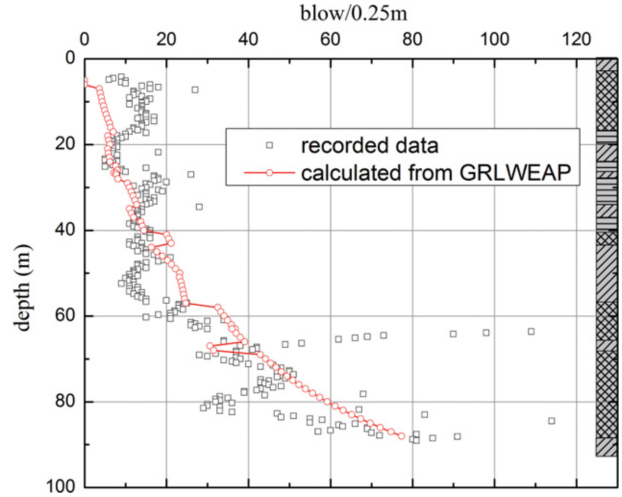

Fig. 4. Blowcount versus depth.

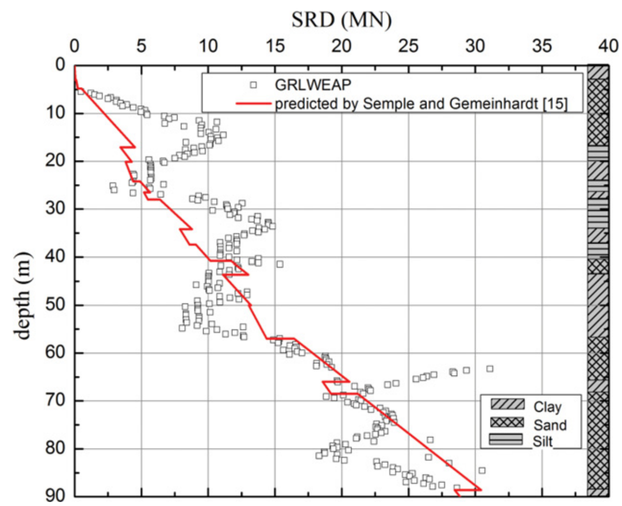

Fig. 5. Soil resistance to driving versus depth.

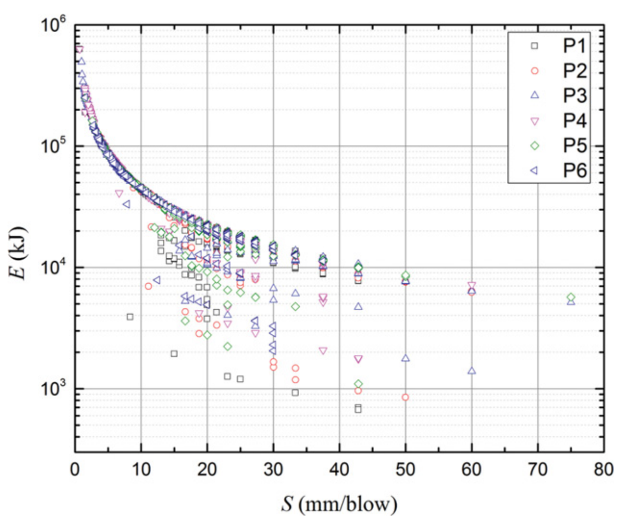

Fig. 6. Blow energy versus settlement.

2.1. Soil profiles

Geotechnical site investigation at the platform location was conducted to collect samples from the boreholes up to 120 m below

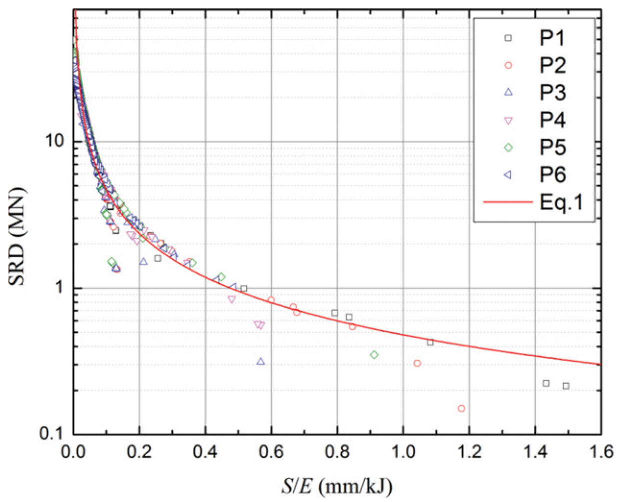

Fig. 7. Soil resistance versus S/E.

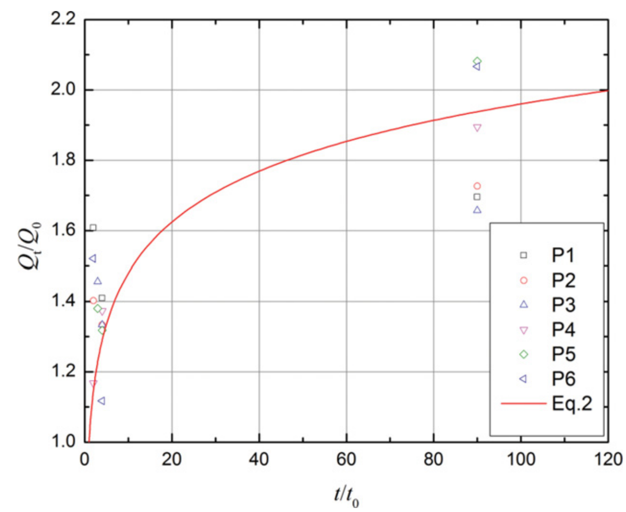

Fig. 8. Time effect on the resistance.

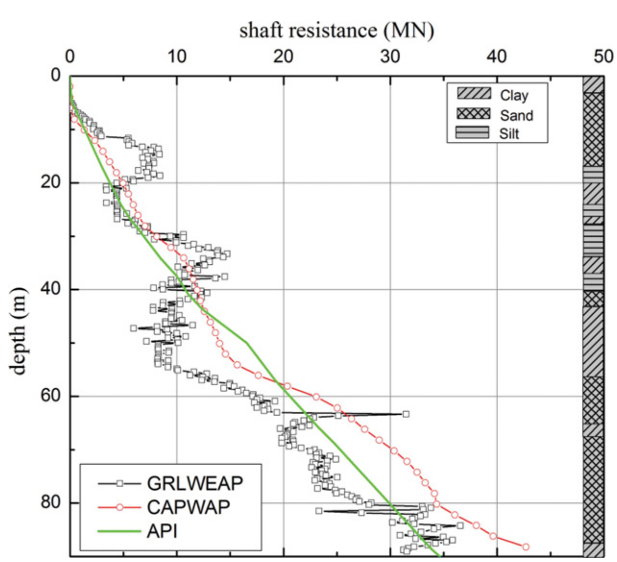

Fig. 9. Shaft friction along the pile.

mudline, which were examined with laboratory testing including unconsolidated undrained triaxial tests, miniature vane and mini penetrometer tests. The soil was found to have 17 layers consisting of

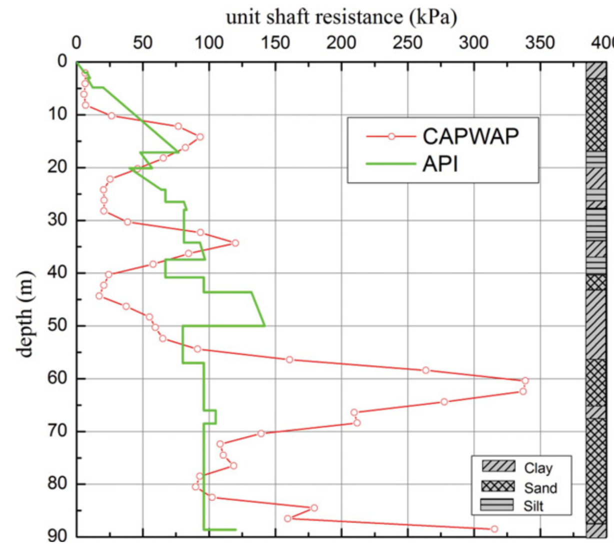

Fig. 10. Unit shaft resistance.

alternating clay, sand and silt. The detailed stratigraphy description (according to Unified Soil Classification System [12]) is shown in Table 1. The undrained shear strength s_u determined from laboratory testing is illustrated in Fig. 1. For better knowledge of the soil, more properties including the unit weight, moisture content and percentage passing 75 μm sieve are shown in Fig. 2.

2.2. *Pile driving and dynamic loading tests*

All the 6 piles are composed of four sections and thus there are three sets of driving pause (interruption) during the pile driving due to welding the pile sections. These driving pauses occur at approximately at 27 m, 63 m and 89 m penetration depth, respectively.

The first three sections of all the 6 piles were driven smoothly using a hydraulic IHC-S-500 hammer with a rated energy of 500 kJ. After three sections, pile driving was suspended for approximately three weeks to set up a larger hammer, i.e. Menck MHU-800 with a rated energy of 800 kJ, which eventually failed to restart the driving. Consequently, a Menck MHU-1200 (with a rated energy of 1200 kJ) hammer was set up after a further four weeks delay. Unfortunately, the MHU-1200 failed to restart driving again. Premature refusals occurred on all the 6 piles at about 89 m penetration depth below mudline.

In order to appraise the bearing capacity of the piles after premature refusal, high strain dynamic load tests were performed about three months after installation of the 3rd sections. MHU-1200 hydraulic hammer was used in the tests to apply the impact force on the pile top to generate stress waves in the tested piles. The signals were recorded by the pile driving analyzer (PDA) and CAPWAP (CAse Pile Wave Analysis Program) [13] analyses were performed to assess the pile capacity.

3. Analysis of pile driving and dynamic loading tests

Wave equation analyses are performed with the software GRLWEAP [14] to study the pile driving and soil resistance. Fig. 3 illustrates the analysis model. Unplugged condition and hydraulic hammer IHC-S-500 are considered in the simulation. Fig. 4 shows the calculated blowcount versus the pile penetration depth. Also shown in the figure is the recorded blowcount (averaged for the 6 piles) during the pile driving. In general, the calculated results agree considerably well with the practical recorded data. This good agreement suggests that simulation with the software GRLWEAP is appropriate to evaluate the piles in this project. Further, the soil shear strength (see Fig. 1) used in this study is able to well represent the soil property. According to

Table 1
Soil layer description.

Layer	Depth (m)	Description	Group symbol
1	0–3	Very soft to soft CLAY	CL
2	3–4.8	Medium dense silty fine SAND	SM
3	4.8–17.1	Very dense fine SAND	SW
4	17.1–20.1	Medium dense sandy SILT	ML
5	20.1–24.2	Firm to stiff silty CLAY	CL
6	24.2–26.5	Medium dense sandy SILT	ML
7	26.5–28	Very stiff CLAY	CH
8	28–34.2	Dense sandy SILT	ML
9	34.2–37.4	Very stiff silty CLAY	CL
10	37.4–40.8	Dense SILT	ML
11	40.8–43.6	Very dense silty fine SAND	SM
12	43.6–57	Very stiff to stiff silty CLAY	CL
13	57–66	Very dense silty fine SAND	SM
14	66–68.5	Very stiff silty CLAY	CL
15	68.5–76.6	Very dense silty fine SAND	SM
16	76.6–88.6	Very dense fine SAND	SW
17	88.6–93	Very stiff silty CLAY	CL

Table 2
Dynamic loading test results.

Pile no.	Pile length (m)	Embedded depth (m)	Settlement per blow (mm)	Bearing capacity (MN)		
				Shaft resistance	End resistance	Total resistance
1	128.4	88.5	1.6	42.7	6.8	49.5
2	127.8	89.8	1	44.2	9.5	53.7
3	128.4	88.4	1.5	45.8	4.9	50.7
4	128.4	88.6	1.8	40.5	8.0	48.5
5	127.8	89.1	2	39.8	8.5	48.3
6	128.4	88.6	1.2	46.0	3.8	49.8
Average	128.2	88.8	1.5	43.2	6.9	50.1

Table 3
Soil resistance and time effect

Pile no.	First pause at 27 m			Second pause at 63 m			Third pause at 88 m		
	$_0$(MN)	Q_t(MN)	t(day)	Q_0(MN)	Q_t(MN)	t(day)	Q_0(MN)	Q_t [a] (MN)	t(day)
P1	4.4	6.2	4	19.4	31.2	2	29.2	49.5	90
P2	5.1	7.8	4	19.4	27.2	2	31.1	53.7	90
P3	5.1	6.8	4	19.3	28.1	3	30.6	50.7	90
P4	6.7	9.2	4	19.1	22.3	2	25.6	48.5	90
P5	4.4	5.8	4	19.2	26.5	3	23.2	48.3	90
P6	9.4	10.5	4	19.2	29.2	2	24.1	49.8	90
Average	5.9	7.7		19.3	27.4		27.3	50.1	

[a] This value is calculated from CAPWAP with the dynamic tests.

the calculated GRLWEAP results, the relationship between blowcount and soil resistance to driving (SRD) can be evaluated by combining the recorded blowcount. Fig. 5 illustrates the calculated SRD along the pile penetration depth. Also shown in Fig. 5 is the prediction of SRD from the Semple and Gemeinhardt approach [15,16]. Close agreement can be seen in Fig. 5 although the Semple and Gemeinhardt approach predicted a smaller value at 5–20 m (mainly very dense fine sand) and a slightly larger value at 45–57 m (very stiff to stiff silty clay).

During pile driving, the hammer impact energy E and the corresponding settlement per blow S were recorded as continuous pile driving data (which is a common practice for the contemporary pile projects). Fig. 6 depictures these recorded data for all the 6 piles (P1–P6). A clear trend between E and S can be observed. In the figure, the low E and large S correspond to low soil resistance while high E and small S denote high soil resistance, which agrees with the results of Lee et al. [17] shown as Eq. (1).

$$R = \frac{W \times H}{S} = \frac{E}{S} = E \cdot S^{-1} = \left(\frac{S}{E}\right)^{-1} \tag{1}$$

where W is the hammer weight, H is the drop height, and R is the soil resistance.

Following Lee et al. [17], the total SRD (cross referring to Fig. 5) and the S/E are plotted in Fig. 7. The below equation is used to fit the relationship between SDR and S/E:

$$SRD = a\left(\frac{S}{E}\right)^{-b} \tag{2}$$

where the coefficients a and b are best fitted as 0.48 and 0.99 in this paper. As the pile driving records are commonly available in contemporary practice, Eq. (2) and Fig. 7 can be considered as a reference to assess the soil resistance.

With the purpose to assess the pile bearing capacity and provide guidance to the next engineering step, dynamic loading tests on the 6 piles were conducted after the occurrence of premature refusal. The dynamic tests and the widely used software CAPWAP were integrated to evaluate the pile capacity. The calculated bearing capacity (including the shaft and base resistance) from CAPWAP is detailed in

Table 2. The settlement per blow in the tests was all about 1.5 mm. According to Rausche et al. [18], more than 2.5 mm settlement per blow was expected to activate full pile capacity. From this point, the real pile bearing capacity of this project is expected to be larger than the calculated value in Table 2.

As aforementioned, the 1st and 2nd driving pauses due to pile section welding occurred at approximately 27 m and 63 m penetration depth (corresponding to layer 7 and 13, see Fig. 1). In this study, the soil resistance corresponding to finishing one pile section is denoted as Q_0 while Q_t represents the soil resistance after a suspension of time t. Table 3 details the Q_0 and Q_t of the 1st and 2nd driving pauses. Also shown in Table 3 is the Q_0 after installing the 3rd pile section (with 88 m depth) and the bearing capacity Q_t evaluated from dynamic test with CAPWAP (3 months later). Skov and Denver [19] proposed an empirical relationship to estimate the time effect on the resistance:

$$\frac{Q_t}{Q_0} = 1 + A\left[\log\left(\frac{t}{t_0}\right)\right] \tag{3}$$

where A and t_0 are two empirical parameters depending on the soil properties [20]. t_0 is commonly considered as 1 day according to Bullock's [21] recommendation. This study's data (Table 2) are plotted as the dots in Fig. 8. The curve of Eq. (2) with a best fitting of the parameter $A = 0.47$ and $t_0 = 1$ day can be obtained from this study's data. We can observe from this figure that the soil resistance increases more rapidly after pile driving than 3 months later.

To further understand the soil setup effect, the shaft resistance is isolated from the total pile. Fig. 9 shows the average shaft resistance calculated from GRLWEAP (while the total SRD is shown in Fig. 5). Also shown in the figure is the shaft resistance derived from dynamic test with CAPWAP. In general, the soil resistance after 3 months (calculated from CAPWAP) is larger than the SRD with exceptional larger SDR can be seen at 5–20 m. This has not been fully understood and may attribute to the conservatism of the dynamic tests due to limit settlement. In addition, the shaft resistance recommended by API 2A [22] is calculated and plotted in the figure, which is based on the soil natural condition (see Fig. 1 and Table 1). A good agreement between API 2A and dynamic loading tests can be seen above 60 m depth. Below 60 m depth the soil is mainly sand (see Fig. 1) and API 2A prediction is slightly lower than CAPWAP. Further, unit shaft resistance of CAPWAP and API is calculated from Fig. 9 as the shaft friction per unit area and shown in Fig. 10. It can be seen more clearly in Fig. 10 that CAPWAP value agrees well with API up to 60 m (mainly clay and silt) but higher than API prediction at deeper penetration.

4. Conclusion

This paper described a practical engineering case associating premature refusal during pile driving in Bohai Bay. The driving records and dynamic tests 3 months after were presented in sufficient details. Based on these data, empirical equations were proposed to evaluate the pile capacity with the data easily to get from driving records. This study is hoped to enrich offshore pile driving experience and shed some light on the pile design, especially for projects with similar soil conditions.

References

[1] Randolph M, Cassidy M, Gourvenec S, Erbrich C. Challenges of offshore geotechnical engineering. In: Proc. 16th international conference on soil mechanics and geotechnical engineering, Osaka. 2005, pp. 123–76.

[2] Puech A, Poulet D, Boisard P. A procedure to evaluate pile drivability in the difficult soil conditions of the southern part of the Gulf of Guinea. In: Proc. offshore technology conference, OTC 6237. Houston. 1990.

[3] Barbour RJ, Erbrich CT. Analysis of in-situ reformation of flattened large diameter foundation piles using ABAQUS. In: Proc. UK ABAQUS users conf. Oxford. 1994.

[4] Alm T, Snell RO, Hampson KM, Olaussen A. Design and installation of the Valhall piggyback structures. In: Proc. offshore technology conference, OTC 16294. Houston. 2004.

[5] Sullivan RA, Ehlers CJ. Practical planning for driving offshore pipe piles. In: Proc. offshore technology conference, OTC 1718. Houston. 1972.

[6] Brunning P, Ishak B. Improved pile driving predictions in carbonate soils and rock. In: Proc. offshore technology conference, OTC 23232. Houston. 2012.

[7] Hussein MH, Woerner WA II, Sharp M, Hwang C. Pile driveability and bearing capacity in high-rebound soils. In: GeoCongress 2006: geotechnical engineering in the information technology age. Atlanta, GA. 2006, pp. 1–4.

[8] Ryzhkov IB, Isaev ON. Application of CPT for adequate selection of pile driving techniques. In: 2nd international symposium on cone penetration testing. 2010.

[9] Schneider JA, White DJ, Kikuchi Y. Analysis of large diameter pipe pile drivability in Tokyo bay using piezocone data. In: Proc. of GeoFlorida 2010, advances in analysis, modeling, and design. Florida. 2010, pp. 1488–97.

[10] Stevens RF. Development of deep foundation design for the offshore environment. In: Proc. of GeoFlorida 2010, advances in analysis, modeling, and design. Florida. 2010, pp. 635–52.

[11] Jardine RJ, Chow FC. Some recent developments in offshore pile design. In: Proc. of the international offshore site investigation and geotechnics conference: confronting new challenge and sharing knowledge. London. 2007, pp. 11–13.

[12] Classification of soils for engineering purposes: annual book of ASTM standards, D2487–11. American Society for Testing and Materials; 2011.

[13] Fellenius BH, Altaee A. Pile dynamics in geotechnical practice—six case histories. In: International deep foundation congress, an international perspective on theory, design, construction, and performance, vol. 2. 2001, pp. 619–31.

[14] Pile Dynamics Inc. (PDI). GRLWEAP—wave equation analysis of pile driving, procedures and models. Cleveland, OH; 2005.

[15] Semple RM, Gemeinhardt JP. Stress history approach to analysis of pile driving. In: Proc. offshore technology conference, OTC 3696. Houston. 1981.

[16] Stevens RF, Wiltsie EA, Turton TH. Evaluating pile driveability for hard clay, very dense sand and rock. In: Proc. offshore technology conference, OTC 7668. Houston. 1982.

[17] Lee LL, James R, Hirsch TJ. A comparison of dynamic pile driving formulas with the wave equation, research report 33–12; 1968.

[18] Rausche F, Nagy M, Likins G. Mastering the art of pile testing. In: The 8th inter. conf. on the application of stress wave theory to piles. Lisbon. 2008, pp. 19–32.

[19] Skov R, Denver H. Time-dependence of bearing capacity of piles. In: Proc. 3rd int. conf. app. stress-wave theory to piles. Ottawa. 1988, pp. 879–88.

[20] Camp WM III, Parmar HS. Characterization of pile capacity with time in the Cooper Marl: a study of the applicability of a past approach to predict long-term pile capacity. TRB 1999:1–19.

[21] Bullock PJ. Pile friction freeze: a field and laboratory study. PhD dissertation. University of Florida; 1999.

[22] API RP 2A. Recommended practice for planning, designing and constructing fixed offshore platforms, USA; 2000.